JACS
JOURNAL OF THE AMERICAN CHEMICAL SOCIETY
Communication
pubs.acs.org/JACS

In Situ Visualization of Self-Assembly of Charged Gold Nanoparticles

Yuzi Liu,* Xiao-Min Lin, Yugang Sun, and Tijana Rajh

Center for Nanoscale Materials, Argonne National Laboratory, 9700 South Cass Avenue, Argonne, Illinios 60439, United States

Supporting Information

ABSTRACT: Self-assembly of Au nanoparticles (NPs) coated with positively charged cetyltrimethylammonium ions (CTA^+) and negatively charged citrate ions in aqueous liquid cell was investigated by in situ transmission electron microscopy (TEM). Under electron illumination in TEM, the hydrated electrons will reduce the overall positive charges of the CTA^+ covered Au NPs and decrease the repulsive electrostatic forces among NPs, leading to assembly of individual NPs into one-dimensional structures. On the contrary, the negatively charged Au NPs coated with citrate ions are steady in liquid cell regardless of electron beam intensity.

Self-assembly of small objects such as atoms, molecules and NPs into mesoscopic structures is a frequently used building approach in material science, biology and chemistry.[1] The self-assembly of NPs attracts great attention for its potential application in the fabrication of hybrid systems with collective properties from different types of materials.[2] There were great efforts devoted to understand the mechanism that governs the self-assembly both from experimental[3] and theoretical[4] approaches. It is now understood that different types of interactions can drive the self-assembly process at nanoscale.[5] This led to formation of variety of self-assembled superstructures with different packing arrangements of individual NPs.[5] Kinetically, the NP assembly process has been monitored by in situ optical spectroscopy and small-angle X-ray scattering (SAXS) techniques.[6] However, optical microscopy has very limited spatial resolution and is unable to resolve individual NPs[6a] and SAXS records data in the reciprocal space and needs complex analysis to obtain real space structural information.[6c] Recently, the development of TEM liquid cells provides a direct imaging platform to visualize the nanoscale objects growth and assembly.[7] The growth of Pt NPs and Pt_3Fe nanorods[7d,8] and oriented attachment of ferrihydrite nanocrystals[9] were imaged recently with in situ liquid TEM. In this paper, we report the high energy electron beam (e-beam) induced self-assembly of Au NPs coated with positive charged CTA^+ and negative charged citrate ions (CI^-) in solution. Because of the difference of surface charge, the Au NPs behave differently as they are illuminated with e-beam. Self-assembly of positively charged Au NPs into 1D chains is observed when the e-beam intensity exceeds a threshold of 5pA/cm^2, while negatively charged particles do not move regardless of the e-beam intensity.

Typical time sequential images of CTA^+ covered Au (CTA-Au) NPs exposed to the e-beam are shown in Figure 1 (see Movie S1 for details). At the beginning of illumination by e-beam, most of the NPs are well separated in the cell because of the electrostatic repulsion between positively charged CTA-Au NPs (Figure 1a). Once the e-beam intensity exceeds the threshold value (i.e., 5 pA/cm^2), CTA-Au NPs begin to detach from the cell window and move in liquid phase freely. The motion eventually leads to particles aggregating into dimers or trimers (Figure 1b,c), and ultimately form 1D structures (Figure 1c–f). The attachment between the short self-assembled chains and that between individual particles and short chains take place simultaneously and the process proceeds

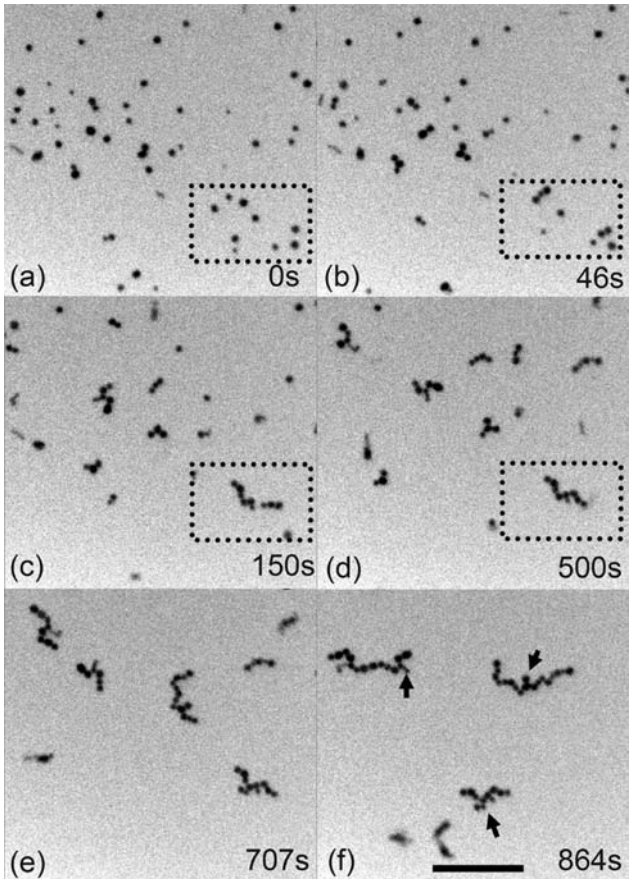

Figure 1. The time sequential images from Movie S1. (a) At the beginning, NPs are well separated; (b) after 150 s illumination by e-beam with intensity of 10pA/cm^2, the dimers, trimers formed; (c and d) the short chains formed by existing dimer, trimer attachment and individual NPs attachment. The scale bar is 500 nm.

Received: December 27, 2012
Published: February 22, 2013

   dx.doi.org/10.1021/ja312620e | J. Am. Chem. Soc. 2013, 135, 3764–3767

until all individual particles are exhausted (Movie S1 and Figure 1f). On the other hand, negative charged citrate coated Au (CI^--Au) NPs of similar sizes show no signs of detachment from the cell wall regardless of e-beam intensity.

The forces among NPs such as van der Waals, electrostatic forces, magnetic forces, molecular surface forces and entropy in the system have been argued as the important factors to control the self-assembly.[5,10] The dipolar interaction is recognized as the dominant control factor in the formation of 1D self-assembly of CdTe NPs[11] and Pt_3Fe nanorods growth[8] because of its anisotropy, high strength, and long-range effect.[12] In our work, the as-prepared CTA-Au NPs are positively charged and repel each other, so what is the transformation created by e-beam that surpasses their repulsion and promotes their aggregation? Since the experiments are performed in the TEM, we first need to consider the global effects of e-beam including momentum transfer, thermal effect, and charging effects. It has been shown that momentum transfer from e-beam to NPs is negligible.[7d] The thermal effect arising from the e-beam heating is minor resulting in only a couple degrees change in temperature.[7d,13] The weak heating effect can be further confirmed by the fact that negatively charged CI^--Au NPs do not move under e-beam, suggesting that thermal effect is not essential in promoting particle motion and self-assembly. These comparisons indicate that the surface charges of NPs may play an important role in the NPs' assembly.

The e-beam used in this work has energy of 200 keV, which is sufficient to promote ionization of the matrix through the electrons pass. It has been reported that there is a positive surface potential developed by the e-beam exposure of insulating TEM foils and the higher beam intensity will generate the larger positive potential.[13,14] This is explained by the balance of the input and output charges on e-beam exposed area (see Supporting Information (SI) for details). This positive electrostatic potential on the cell membranes will repel positively charged CTA-Au NPs initially attached to the cell window, causing their migration into the liquid. On the other hand, CI^--Au NPs stick to cell window. There are reactive hydrated electrons formed by the interaction of 200 keV e-beam with water.[7d,15] Recent work shows such hydrated electrons are capable of reducing platinum ions to grow Pt NPs.[7d] In our case, hydrated electrons are reacting with Au NPs[16] diminishing the overall positive charge of CTA-Au NPs. As a result, the electrostatic repulsion among the CTA-Au NPs is reduced and the NPs can encounter each other to form dimers. Electrons injected into Au NP most likely thermalize onto the trapping sites producing polaron-like states. Transient polaron-like states were previously observed upon interaction of Au NP with light.[17] In our experiment, polaron like states will persist as long as electron scavengers are absent. Concomitantly, the dipole moment developed between polaronic states and charged polymer will promote ordering of NPs. Once the dimers are formed, the stronger dipole will be generated. Consequently, there will be a stronger anisotropic energy that drives an extra particle to attach to the end of a chain.[12a] The strong anisotropic dipolar interaction between dimers, trimers will foster formation of longer chains. In addition to the dipolar interaction mechanism, once the dimer is formed, they effectively behave like rods. van der Waals attractive interaction between a sphere and a rod could also favor 1D attachment.[18] It should be noted that electrostatic self-assembly approach developed by Grzybowski et al.[19] was employed for the growth of binary NP crystals or variety of NP supercrystals. Similar effects were also obtained by controlled change of the ionic strength of colloidal solution confirming that neutralization of charge of NPs results in the assembling of NPs (as shown in Figures S3 and S4). However, the neutralization in both of these cases involves only surfactant molecules and the self-assembled objects do not grow anisotropically, but equally in all directions.

One advantage of in situ measurement is the ability to track the motion of individual NPs. Figure 2a shows the trajectories

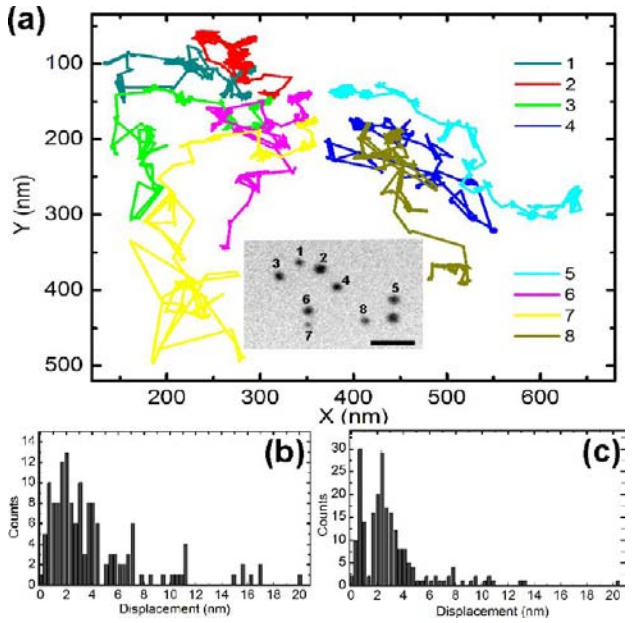

Figure 2. Analysis of Au NPs motion. (a) Trajectories of 8 NPs showing in inset (scale bar 200 nm) participate the assembly. (b and c) Histograms showing the distribution of displacement at each time step of 0.4 s of the 30 and 50 nm Au NP over time span of 400 s, respectively.

of eight different NPs during the e-beam induced assembly from a boxed rectangular region in Figure 1. The two-dimensional center-of-particle position $P(r_i) = [x_i, y_i]$ in each frame is obtained with an accuracy of 0.5 nm and a time step of 0.4 s. To investigate the movement of individual particles, the histograms of displacement of 30 and 50 nm-NPs at a time step of 0.4 s are plotted in Figure 2b and c, respectively (data extracted from trajectories 7 and 8 in Figure 2a). It can be seen that both the small and large steps coexist in single NP's motion (see detail in Movie S2). On average, the small particle displacements are larger than the big ones and the displacement distribution is qualitatively more scattered than that of large ones. We find usually there are bigger displacements just prior to the attachment (Movie S2). This suggests that the movement of the NPs accelerates in the vicinity of other NPs, confirming the existence of an attractive field that assists the NPs to overcome the energy barrier that blocks the attachment between NPs.

We also found the beam intensity has critical effect on self-assembly. The results show that the movement of CTA-Au NPs depends on e-beam intensity. CTA-Au NPs do not move at low beam intensity (<5pA/cm2) and they are more agile under the beam of stronger intensity (see detail in Movie S3). When a mixture of NPs with different sizes of 20 and 45 nm (Figure S5) is exposed to e-beam, smaller sized NPs self-assembled first. In

dx.doi.org/10.1021/ja312620e | J. Am. Chem. Soc. 2013, 135, 3764−3767

addition, we find that NPs of the certain size only self-assembled with particles of similar size into separate chains, as indicated by arrows in Figure 3. The fact that small NPs move

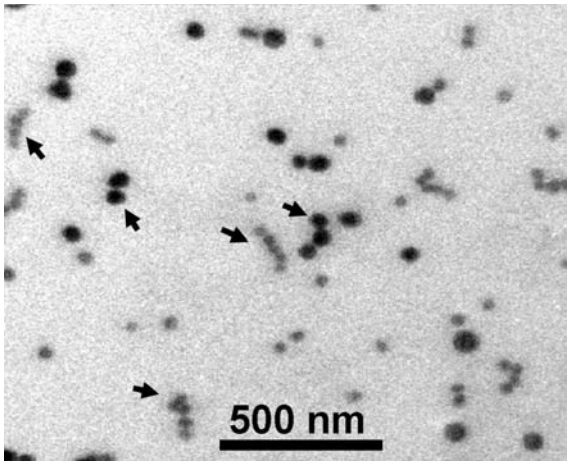

Figure 3. The snapshot of the end of Movie S3 showing the self-assembly of CTA-Au NPs with similar size.

faster and have larger moving step size compared to the big ones enables them to encounter other small NPs more frequently. A slight difference of contrast in bright field images indicates different sizes of particles might reside at different depths in liquid cell. The reason for NPs' segregation lies in the surface potential of the liquid cell windows and different charge condition between the small and big particles. As mentioned earlier, the higher beam intensity will generate the larger positive potential in Si_3N_4 foil.[13,14] We can expect qualitatively that under the beam intensity >5pA/cm^2, the significant positive potential will be developed. This large positive potential will result in the repelling force between positively charged CTA-Au NPs and positive Si_3N_4 membranes. The e-beam effects more significantly on the top Si_3N_4 window than the bottom one as the amount of electrons that reach the bottom window becomes attenuated by the first window and the NP solution. As a result, a voltage gradient develops and NPs start moving according to their mass and their surface charge. Consequently, small and large particles segregate at a different depth of a liquid cell fostering self-assembly of alike molecules. Alternatively, the size selected self-assembly might also be caused by the size dependence of the dispersional attractions which are strong enough to dominate over entropic effects.[17]

To understand which of these mechanisms is responsible for segregation of NPs, we disassembled the liquid cell which was used to record Movie S3. Then, both Si_3N_4 membranes were loaded back to TEM, and bright field images of the same areas as those used during in situ experiment were obtained (Figure 4 and Figure S5). We found that aggregates of small size Au NPs are placed only on top Si_3N_4 membrane and aggregates of large NPs are found on bottom Si_3N_4 membrane only (Figure S5). This indeed confirmed that during the in situ experiment, NPs with different sizes are separated at different heights of a liquid cell and do not have the opportunity to meet with each other. Therefore, segregation of NP observed in NPs is not a consequence of size selected self-assembly but due to the electrophoretic separation of NPs in the electric field. These

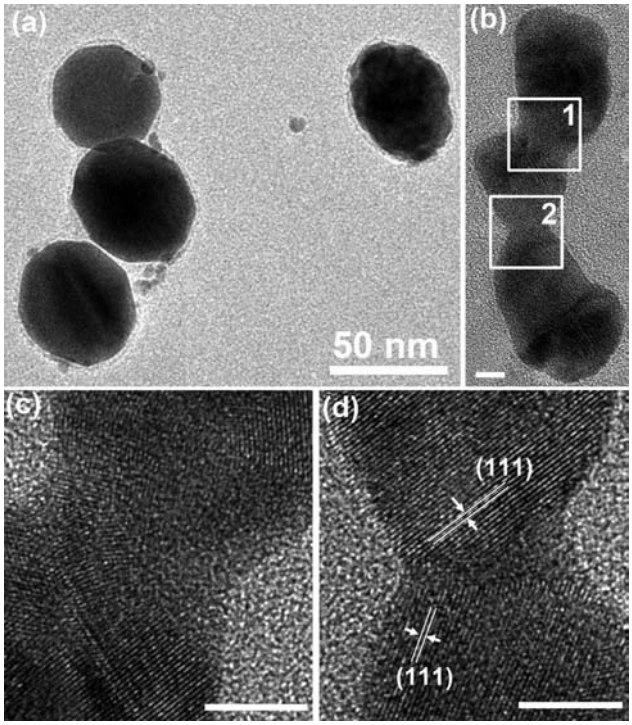

Figure 4. TEM micrograph of dried liquid cell used to record Movie S3. (a) Trimer formed with ~45 nm particles; (b) object formed by ~20 nm particles; (c and d) HREM images of profiles 1 and 2 in (b). Scale bar in b–d is 10 nm.

findings suggest a new approach for creating size selected self-assembly.

Careful investigation of ex situ images also shows that there is a perfect low contrast layer of CTA^+ on the surface of the trimer assembled from ~45 nm NPs (Figure 4a). On the other hand, there is no such clear layer on the surface of the sintered object assembled by ~20 nm NPs, as shown in Figure 4b. From the HREM images of Figure 4c,d, which correspond to the profiles 1 and 2 in Figure 4b, respectively, we can see the clear sintering of the two particles. In contrast, there is no such interdiffusion between the 45 nm NPs as shown in Figure 4a. We believe that because of the smaller surface energy and the smaller surface curvature of the large particles, there would be a more ordered and denser, and therefore more stable, CTA^+ layer on big NPs than that of the small ones.[20] Moreover, the hydrated electrons will reduce the overall positive charge of small CTA-Au particles faster than the big CTA-Au NPs because smaller NPs have lower number of CTA^+ per Au particle. In addition, the small particles have larger diffusion coefficient than the big ones in solution and have larger probability of reacting with hydrated electrons and another NP.[21] This is evident from the fact that the small particles form dimer first in the early stage of assembly, as shown in Movie S3. The stable CTA^+ layers on large NPs will block Au atoms interdiffusion and leave the gap as shown in Figure 4a. In comparison, CTA^+ can be easily rearranged at the surface of small NPs permitting close encounter of small NPs and interdiffusion of Au atoms. It should be noted that the concentration of NPs with different size might also affect the encounter probabilities of NPs. But the concentration of ~20 and ~45 nm-NPs is almost same in our view area of Movie S3.

In conclusion, 1D chain forming by CTA-Au NPs was observed by in situ liquid TEM technique. The hydrated

dx.doi.org/10.1021/ja312620e | J. Am. Chem. Soc. 2013, 135, 3764–3767

electrons formed as radiolysis of water decreased the overall positive charge of CTA-Au NPs. The anisotropic attractive interactions, including dipole−dipole interaction and van der Waals interaction, overcome the repulsion among the NPs and induce the assembly of NPs in a 1D chain. We also found evidence of spatial segregation of different sizes of NPs as a result of electric field gradient within the cell. These observations, on one hand, clearly elucidated the complex mechanism of charged NP self-assembly process, but on the other, paint a cautionary picture on using TEM in situ cell to imitate self-assembly processes in a real solution environment.

■ ASSOCIATED CONTENT

Supporting Information

The liquid cell fabrication; data processing; ζ-potential characterization; absorption spectra; dried Au NPs TEM images. This material is available free of charge via the Internet at http://pubs.acs.org.

■ AUTHOR INFORMATION

Corresponding Author

yuziliu@anl.gov

Notes

The authors declare no competing financial interest.

■ ACKNOWLEDGMENTS

This work was performed at the Center for Nanoscale Materials, a U.S. Department of Energy, Office of Science, Office of Basic Energy Sciences User Facility under Contract No. DE-AC02-06CH11357. The authors thank Sergey Chemerisov for experiments using Van de Graaff accelerator.

■ REFERENCES

(1) (a) Shenton, W.; Pum, D.; Sleytr, U.; Mann, S. *Nature* **1997**, *389*, 585. (b) Guarini, K. W.; Black, C. T.; Yeung, S. H. I. *Adv. Mater.* **2002**, *14*, 1290. (c) Redl, F. X.; Cho, K. S.; Murray, C. B.; O'Brien, S. *Nature* **2003**, *423*, 968. (d) Shevchenko, E. V. *J. Am. Chem. Soc.* **2002**, *124*, 11480.

(2) (a) Robel, I.; Bunker, B. A.; Kamat, P. V. *Adv. Mater.* **2005**, *17*, 2458. (b) Nie, Z.; Petukhova, A.; Kumacheva, E. *Nat. Nano* **2010**, *5*, 15. (c) Hirakawa, T.; Kamat, P. V. *J. Am. Chem. Soc.* **2005**, *127*, 3928.

(3) (a) Boal, A. K.; Ilhan, F.; DeRouchey, J. E.; Thurn-Albrecht, T.; Russell, T. P.; Rotello, V. M. *Nature* **2000**, *404*, 746. (b) Yang, J.; Elim, H. I.; Zhang, Q.; Lee, J. Y.; Ji, W. *J. Am. Chem. Soc.* **2006**, *128*, 11921. (c) Shevchenko, E. V.; Talapin, D. V.; O'Brien, S.; Murray, C. B. *J. Am. Chem. Soc.* **2005**, *127*, 8741. (d) Nikoobakht, B.; Wang, Z. L.; El-Sayed, M. A. J. *Phys. Chem. B* **2000**, *104*, 8635.

(4) (a) Lane, J. M. D.; Grest, G. S. *Phys. Rev. Lett.* **2010**, *104*, 235501. (b) Khan, S. J.; Pierce, F.; Sorensen, C. M.; Chakrabarti, A. *Langmuir* **2009**, *25*, 13861. (c) Rabani, E.; Reichman, D. R.; Geissler, P. L.; Brus, L. E. *Nature* **2003**, *426*, 271. (d) Luo, M.; Mazyar, O. A.; Zhu, Q.; Vaughn, M. W.; Hase, W. L.; Dai, L. L. *Langmuir* **2006**, *22*, 6385. (e) Luo, M.; Dai, L. L. *J. Phys.: Condens. Matter.* **2007**, *19*, 375109.

(5) Bishop, K. J. M.; Wilmer, C. E.; Soh, S.; Grzybowski, B. A. *Small* **2009**, *5*, 1600.

(6) (a) Bigioni, T. P.; Lin, X.-M.; Nguyen, T. T.; Corwin, E. I.; Witten, T. A.; Jaeger, H. M. *Nat. Mater.* **2006**, *5*, 265. (b) Jiang, Z.; Lin, X.-M.; Sprung, M.; Narayanan, S.; Wang, J. *Nano Lett.* **2010**, *10*, 799. (c) Narayanan, S.; Wang, J.; Lin, X.-M. *Phys. Rev. Lett.* **2004**, *93*, 135503. (d) Wang, Y.; DePrince, A. E.; K. Gray, S.; Lin, X.-M.; Pelton, M. *J. Phys. Chem. Lett.* **2010**, *1*, 2692. (e) Beale, A. M.; O'Brien, M. G.; Kasunic, M.; Golobic, A.; Sanchez-Sanchez, M.; Lobo, A. J. W.; Lewis, D. W.; Wragg, D. S.; Nikitenko, S.; Bras, W.; Weckhuysen, B. M. *J. Phys. Chem. C* **2011**, *115*, 6331.

(7) (a) Williamson, M. J.; Tromp, R. M.; Vereecken, P. M.; Hull, R.; Ross, F. M. *Nat. Mater.* **2003**, *2*, 532. (b) de Jonge, N.; Ross, F. M. *Nat. Nano* **2011**, *6*, 695. (c) Jonge, N. d.; Peckys, D. B.; Kremers, G. J.; Piston, D. W. *Proc. Natl. Acad. Sci. U.S.A.* **2009**, *106*, 2159. (d) Zheng, H.; Smith, R. K.; Jun, Y.-w.; Kisielowski, C.; Dahmen, U.; Alivisatos, A. P. *Science* **2009**, *324*, 1309.

(8) Liao, H.-G.; Cui, L.; Whitelam, S.; Zheng, H. *Science* **2012**, *336*, 1011.

(9) Li, D.; Nielsen, M. H.; Lee, J. R. I.; Frandsen, C.; Banfield, J. F.; De Yoreo, J. J. *Science* **2012**, *336*, 1014.

(10) (a) Ku, J.; Aruguete, D. M.; Alivisatos, A. P.; Geissler, P. L. *J. Am. Chem. Soc.* **2010**, *133*, 838. (b) Kolny, J.; Kornowski, A.; Weller, H. *Nano Lett.* **2002**, *2*, 361. (c) Tripp, S. L.; Pusztay, S. V.; Ribbe, A. E.; Wei, A. *J. Am. Chem. Soc.* **2002**, *124*, 7914. (d) Chen, J.; Dong, A.; Cai, J.; Ye, X.; Kang, Y.; Kikkawa, J. M.; Murray, C. B. *Nano Lett.* **2010**, *10*, 5103. (e) Adams, M.; Dogic, Z.; Keller, S. L.; Fraden, S. *Nature* **1998**, *393*, 349. (f) Koenderink, G. H.; Vliegenthart, G. A.; Kluijtmans, S. G. J. M.; van Blaaderen, A.; Philipse, A. P.; Lekkerkerker, H. N. W. *Langmuir* **1999**, *15*, 4693. (g) Asakura, S.; Oosawa, F. J. *Polym. Sci.* **1958**, *33*, 183. (h) Sau, T. K.; Murphy, C. J. *Langmuir* **2005**, *21*, 2923.

(11) Tang, Z.; Kotov, N. A.; Giersig, M. *Science* **2002**, *297*, 237.

(12) (a) Rajh, T.; Thurnauer, M. C.; Thiyagarajan, P.; Tiede, D. M. *J. Phys. Chem. B* **1999**, *103*, 2172. (b) Zhang, H.; Wang, D. *Angew. Chem., Int. Ed.* **2008**, *47*, 3984.

(13) Egerton, R. F.; Li, P.; Malac, M. *Micron* **2004**, *35*, 399.

(14) Cazaux, J. *Ultramicroscopy* **1995**, *60*, 411.

(15) Hart, E. J. *Science* **1964**, *146*, 19.

(16) Abidi, W.; Selvakannan, P. R.; Guillet, Y.; Lampre, I.; Beaunier, P.; Pansu, B.; Palpant, B.; Remita, H. *J. Phys. Chem. C* **2010**, *114*, 14794.

(17) Nakanishi, H.; Bishop, K. J. M.; Kowalczyk, B.; Nitzan, A.; Weiss, E. A.; Tretiakov, K. V.; Apodaca, M. M.; Klajn, R.; Stoddart, J. F.; Grzybowski, B. A. *Nature* **2009**, *460*, 371.

(18) He, W.; Lin, J.; Wang, B.; Tuo, S.; Pantelides, S. T.; Dickerson, J. H. *Phys. Chem. Chem. Phys.* **2012**, *14*, 4548.

(19) (a) Kalsin, A. M.; Fialkowski, M.; Paszewski, M.; Smoukov, S. K.; Bishop, K. J. M.; Grzybowski, B. A. *Science* **2006**, *312*, 420. (b) Klajn, R.; Bishop, K. J. M.; Fialkowski, M.; Paszewski, M.; Campbell, C. J.; Gray, T. P.; Grzybowski, B. A. *Science* **2007**, *316*, 261. (c) Walker, D. A.; Kowalczyk, B.; de la Cruz, M. O.; Grzybowski, B. A. *Nanoscale* **2011**, *3*, 1316. (d) Grzybowski, B. A.; Winkleman, A.; Wiles, J. A.; Brumer, Y.; Whitesides, G. M. *Nat. Mater.* **2003**, *2*, 241.

(20) (a) Wang, D.; Nap, R. J.; Lagzi, I. n.; Kowalczyk, B.; Han, S.; Grzybowski, B. A.; Szleifer, I. *J. Am. Chem. Soc.* **2011**, *133*, 2192. (b) Browne, K. P.; Grzybowski, B. A. *Langmuir* **2010**, *27*, 1246.

(21) Zheng, H.; Claridge, S. A.; Minor, A. M.; Alivisatos, A. P.; Dahmen, U. *Nano Lett.* **2009**, *9*, 2460.